Flexible graphite under repeated compression studied by electrical resistance measurements

Xiangcheng Luo, D.D.L. Chung[*]

Department of Mechanical and Aerospace Engineering, Composite Materials Research Laboratory,
State University of New York at Buffalo, Buffalo, NY 14260-4400, USA

Abstract

Flexible graphite (a gasket material) under repeated compression was studied by real-time measurement of the electrical resistance perpendicular to the flexible graphite sheet, which was sandwiched by copper. The resistance decreased reversibly upon compression perpendicular to the sheet, due mainly to the reversible conformability of flexible graphite and the consequent reversible decrease of the contact resistivity between flexible graphite and copper. Two cycles of compression largely eliminated the irreversible resistance and strain changes. A low stress amplitude (<4 MPa) and a low strain amplitude (<25%) were necessary in order to minimize irreversible deformation of the flexible graphite itself. © 2001 Elsevier Science Ltd. All rights reserved.

1. Introduction

Flexible graphite is a flexible sheet made by compressing a collection of exfoliated graphite flakes without a binder [1–11]. Due to the exfoliation, flexible graphite has a large specific surface area (e.g., 15 m^2/g [12]). As a result, flexible graphite is used as an adsorption substrate. Due to the absence of a binder, flexible graphite is essentially entirely graphite (other than the residual amount of intercalate in the exfoliated graphite). As a result, flexible graphite is chemically and thermally resistant, and low in coefficient of thermal expansion (CTE). Due to its microstructure involving graphite layers that are preferentially parallel to the surface of the sheet, flexible graphite is high in electrical and thermal conductivities in the plane of the sheet. Due to the graphite layers being somewhat connected perpendicular to the sheet (i.e., the honeycomb microstructure of exfoliated graphite), flexible graphite is

electrically and thermally conductive in the direction perpendicular to the sheet (although not as conductive as the plane of the sheet). These in-plane and out-of-plane microstructures result in resilience and impermeability to fluids perpendicular to the sheet. The combination of resilience, impermeability and chemical and thermal resistance makes flexible graphite attractive for use as a gasket material for high temperature or chemically harsh environments.

Resilience in terms of the dimensional change upon compression being reversible is key to the repeated use of flexible graphite as a gasket material. Conformability in terms of the surface topography being able to conform in a reversible fashion is also important. Much more attention has been given to the resilience than to the conformability of flexible graphite.

Previous work in characterizing the gasketing ability of flexible graphite mainly involved mechanical and leakage tests [3–11,13–27]. In contrast, this work used electrical resistance measurement during repeated compression to characterize flexible graphite. As the resistance was in the through-thickness direction and included the contact resistance between the flexible graphite and each of the two metal surfaces sandwiching it, the measurement provided information on the conformability of flexible graphite.

*Corresponding author. Tel.: +1-716-645-2593; fax: +1-716-645-3875.

E-mail address: ddlchung@acsu.buffalo.edu (D.D.L. Chung).

2. Experimental methods

Flexible graphite sheets (Grade GTB, EGC Enterprises, Inc., Mentor, OH) of thicknesses 1.6 and 3.1 mm had electrical resistivity 7.5×10^{-4} Ω.cm in the plane of the sheet; that perpendicular to the sheet is 0.011 ± 0.001 and 0.037 ± 0.011 Ω.cm for thicknesses 1.6 and 3.1 mm respectively.

A rectangular piece of flexible graphite was sandwiched between two copper cylinders (diameter=12.8 mm, height=9.9 mm, mechanically polished by using 200-grit sandpaper) labeled B and C (Fig. 1). Two larger pieces of flexible graphite cut from the original sheet (thus same thickness) as the above-mentioned smaller piece were sandwiched between copper cylinders A and B and between copper cylinders C and D. These larger pieces extended beyond the circumference of the copper cylinders, whereas the smaller piece was within the circumference. Silver paint was applied at the interface between each piece of graphite and its adjacent cylinder. A copper wire was soldered to each of the four cylinders. The wires to A and D were for current (DC) to pass, whereas those to B and C were for voltage measurement. The resistance between B and C thus measured consisted of the volume resistance of the graphite between B and C along the cylinder axis and the contact resistance at each of the two interfaces between cylinder (B or C) and graphite (be-

tween B and C), as the volume resistance of each cylinder is negligible. This resistance measurement was conducted while cyclic compression (load control, crosshead speed 0.5 mm/min, screw-action mechanical testing system, Sintech 2/D, Sintech, Stoughton, MA) was applied along the cylinder axis. The strain of the graphite between B and C along the cylinder axis was obtained by dividing the crosshead movement of the mechanical testing system by 1.83, as the stack contained three graphite pieces and the graphite area between B and C was about half of the cylinder area. The graphite strain was directly related to the displacement (change in height of sandwich).

3. Results and discussion

Fig. 2 shows the fractional increase in resistance ($\Delta R / R_o$, negative for decrease), strain (negative for shrinkage) and stress (negative for compression) simultaneously obtained during the first 10 loading cycles at a constant stress amplitude of -0.42 MPa for a flexible graphite sample (7.6×7.1 mm) of thickness 1.60 mm. The resistance (initially being 0.27 Ω) decreased during loading and increased during subsequent unloading in every cycle, such that the resistance change was mostly reversible, but had an irreversible portion at the end of the first cycle. Furthermore, the maximum magnitude of $\Delta R / R_o$ was larger in the first cycle than in subsequent cycles. The irreversible portion at the end of a cycle slightly increased after the subsequent cycle, but did not further change after that. Thus, it took 2 cycles for the cyclic resistance change to stabilize. When stabilized, the magnitude of the reversible portion of $\Delta R / R_o$ was 41%, while the magnitude of the irreversible portion of $\Delta R / R_o$ was 12%. The magnitude of strain increased with the magnitude of stress during each loading, such that the strain magnitude increase was partly reversible and partly irreversible at the end of the first cycle. Moreover, the maximum magnitude of strain was larger in the first cycle than in subsequent cycles. The irreversible portion of strain did not further increase in subsequent cycles. Thus, it took only 1 cycle for the cyclic strain change to stabilize. When stabilized, the magnitude of the reversible portion of strain was 7%, while the magnitude of the irreversible portion of strain was 8%. The $\Delta R / R_o$ variation closely corresponded to the strain variation, such that: (i) a larger magnitude of $\Delta R / R_o$ was associated with a larger magnitude of strain, (ii) the irreversible portion of $\Delta R / R_o$ was associated with the irreversible portion of strain, and (iii) the reversible portion of $\Delta R / R_o$ was associated with the reversible portion of strain. After the initial two loading cycles, the flexible graphite behaved reversibly.

Fig. 3 shows similar results for the same sample and stress amplitude as Fig. 2, but right after the first 10 cycles (shown in Fig. 2), at which the resistance was 0.23 Ω (compared to 0.27 Ω before any cycling). The fractional
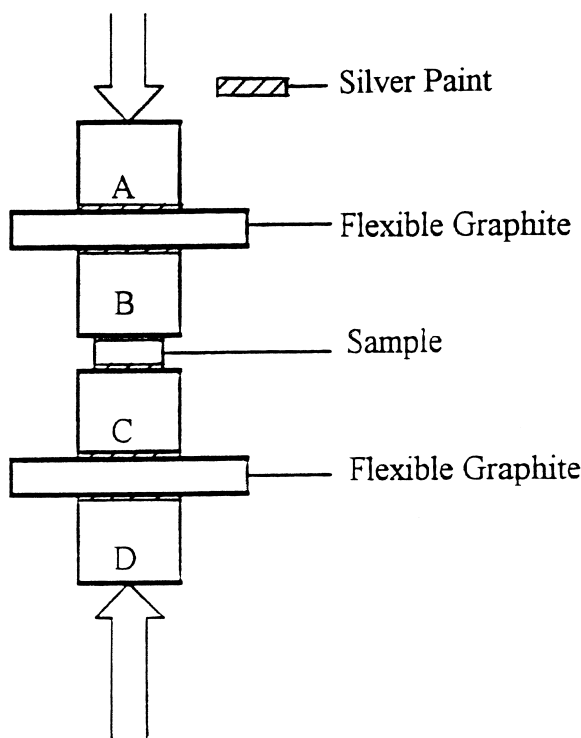

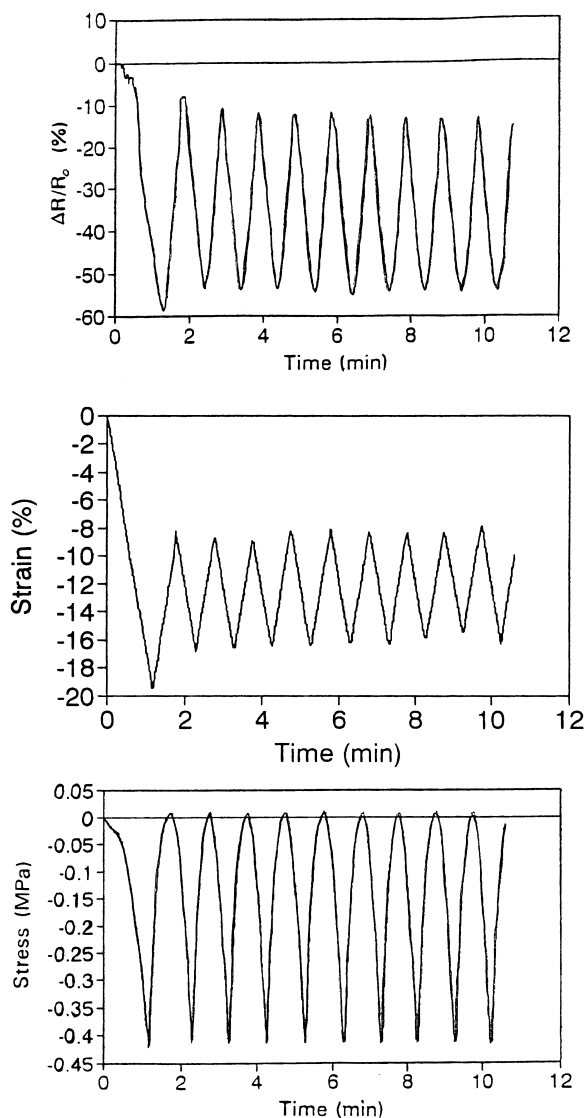Fig. 1. Set-up for electrical resistance measurement.

Fig. 2. Fractional resistance increase ($\Delta R/R_o$), strain and stress simultaneously obtained during the first 10 compressive loading cycles (under load control) of flexible graphite of thickness 1.6 mm and initial resistance 0.27 Ω. The stress amplitude was −0.42 MPa.
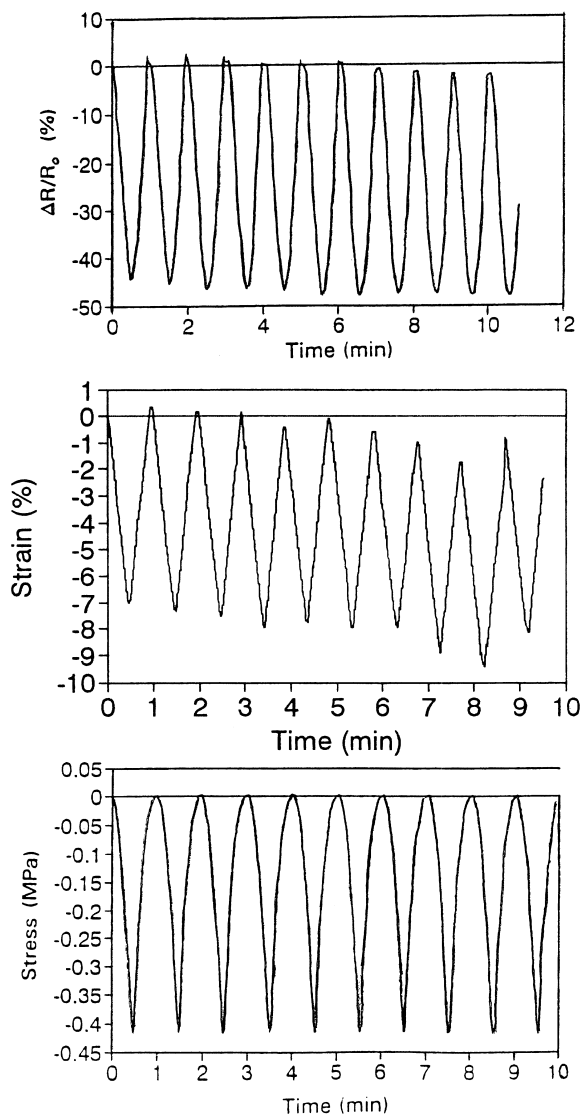
Fig. 3. Fractional resistance increase ($\Delta R/R_o$), strain and stress simultaneously obtained during the first 11 compressive loading cycles (under load control) of flexible graphite of thickness 1.6 mm and initial resistance 0.23 Ω. The sample had been prior stress cycled (as shown in Fig. 2) for stabilization. The stress amplitude was −0.42 MPa.

changes ($\Delta R/R_o$ and strain) shown in Fig. 3 are relative to the values right after the first 10 cycles. Thus, Fig. 3 displays the behavior of flexible graphite which had been stabilized — a situation which is practically useful. In this situation, a reversible stress of −0.42 MPa gave rise to a reversible strain of −7% and a reversible $\Delta R/R_o$ of −43%.

Fig. 4 shows results obtained on the same sample as Figs. 2 and 3, but at a stress amplitude of −0.83 MPa and with a starting point which was right at the end of the cycling in Fig. 3. At this starting point, R was 0.22 Ω. Fig.

4, as Fig. 3, displays the behavior of flexible graphite which had been stabilized. In Fig. 4, a reversible stress of −0.83 MPa gave rise to a reversible strain of −11% and a reversible $\Delta R/R_o$ of −60%.

Similar results were obtained with the same sample as Figs. 2–4, but at stress amplitudes of −1.25, −2.06 and −2.48 MPa. The corresponding reversible $\Delta R/R_o$ was −68%, −70% and −72% respectively; the corresponding reversible strain was −13%, −17% and −19% respectively.
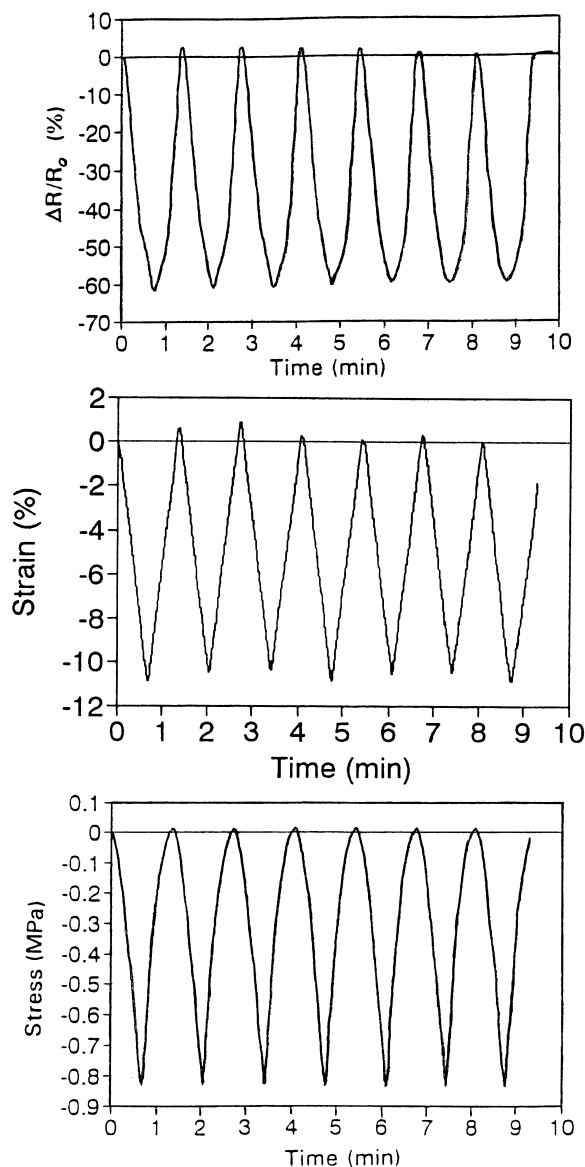
Fig. 4. Fractional resistance increase ($\Delta R/R_o$), strain and stress simultaneously obtained during the first 7 compressive loading cycles (under load control) of flexible graphite of thickness 1.6 mm and initial resistance 0.22 Ω. The sample had been prior stress cycled (as shown in Fig. 2 and 3) for stabilization. The stress amplitude was −0.83 MPa.
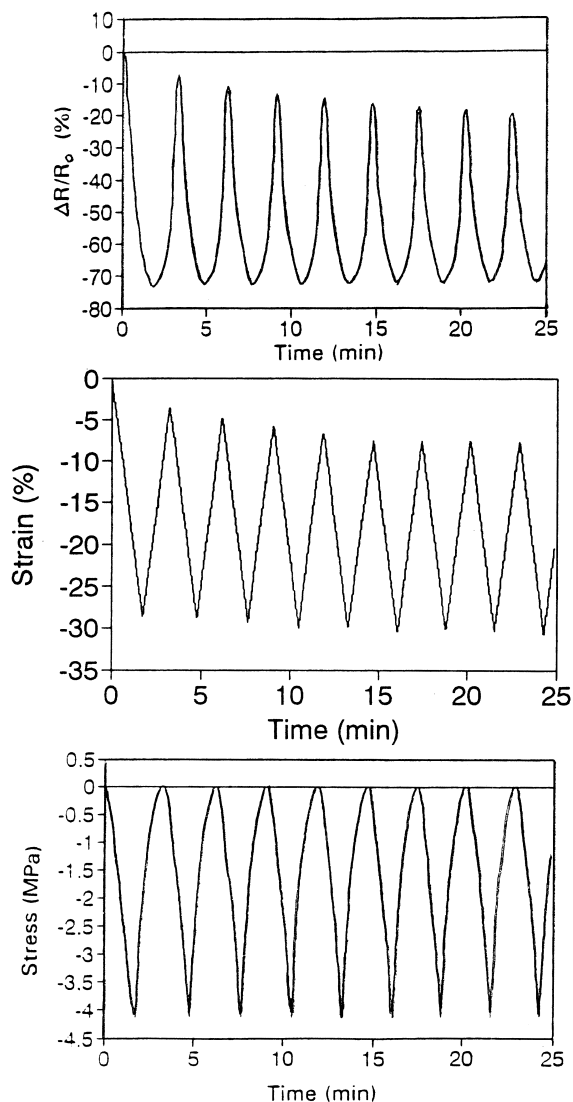

Fig. 5. Fractional resistance increase ($\Delta R/R_o$), strain and stress simultaneously obtained during the first 9 compressive loading cycles (under load control) of flexible graphite of thickness 1.6 mm and initial resistance 0.19 Ω. The sample had been prior stress cycled (as shown in Figs. 2–4) for stabilization. The stress amplitude was −4.12 MPa.

When the stress amplitude reached −4.12 MPa, the irreversible portion of the $\Delta R/R_o$ magnitude as well as that of the strain magnitude increased after every cycle and the maximum strain magnitude (most negative strain) of a cycle increased in every cycle, as shown in Fig. 5. This is due to irreversible shrinkage of the flexible graphite in every cycle at the large stress amplitude. Similar behavior was observed at a stress amplitude of −5.78 MPa. Flexible graphite could not serve as a reliable and reusable gasket when the stress magnitude exceeded 4 MPa or when the strain magnitude exceeded 25%.

When the initial resistance was too high, the $\Delta R/R_o$ and strain changes had significant irreversible portions, even after considerable prior cycling. Therefore, a small initial resistance is preferred. This dependence on the initial resistance is attributed to the fact that the contact resistance between sample and the copper cylinder is an important part of the measured resistance. As shown by calculation of the volume resistance of the sample based on the

Table 1
Initial electrical resistance for various combinations of flexible graphite thickness and stress amplitude

Thickness (mm)	Initial resistance (Ω)	Fraction of initial resistance due to volume resistance	Stress amplitude (MPa)
1.6	0.042	0.079[a]	−0.12
1.6	0.051	0.065[a]	−0.172
1.6	0.27	0.012[a]	−0.42
1.6	0.36	0.009[a]	−0.11
3.1	0.034	0.58[b]	−0.076
3.1	0.084	0.23[b]	−0.166
3.1	0.106	0.18[b]	−0.24

[a] Volume resistance = 0.0033 Ω, as calculated from volume resistivity and sample dimensions.
[b] Volume resistance = 0.020 Ω, as calculated from volume resistivity and sample dimensions.

separately measured volume resistivity perpendicular to the sheet, the volume resistance constitutes only a small part of the measured resistance for most of the samples (Table 1). A low initial resistance reflects mainly a low contact resistance. The contact resistivity varies from one sample to another, while the volume resistivity variation is much smaller. The observed reversible resistance decrease in most of the samples is mainly due to a decrease in the contact resistivity, associated with reversible conforming of the flexible graphite surface to the surface topography of the copper cylinder upon compression. The reversibility is possibly due to the resilience of flexible graphite. The contributions to the observed resistance decrease by a possible reversible resistivity decrease (microstructural change) in the flexible graphite upon compression and by the thickness decrease are small in most of the samples. A high initial resistance corresponds to a high contact resistivity (i.e., a poor interface), which in turn corresponds to a large irreversible portion of $\Delta R/R_o$ (associated with some irreversible tendency to conform to the surface topography of the copper cylinder). The irreversible $\Delta R/R_o$ corresponds to irreversible strain, which is −8% in Fig. 2. The irreversible strain is associated partly with the irreversible tendency to conform to the surface topography of the copper cylinder and partly with irreversible thickness decrease.

4. Conclusion

The electrical resistance perpendicular to the flexible graphite sheet (sandwiched by copper) decreased reversibly upon compressive loading perpendicular to the sheet, due mainly to the reversible conformability of flexible graphite and the consequent reversible decrease of the contact resistivity between flexible graphite and copper. Two cycles of compression largely eliminated the irreversible resistance and strain changes. A low stress amplitude (<4

MPa) and a low strain amplitude (<25%) were necessary in order to minimize irreversible deformation of the flexible graphite itself.

References

[1] Shane JH, Russell RJ, Bochman RA. Flexible graphite materials of expanded particles compressed together. US Patent 3 404 061, 1968.

[2] Flitney FK. Soft packings. Tribology Int 1986;19:181.

[3] Derenne M, Marchand L, Payne JR. Characterization behaviour of flexible graphite sheet gasket materials. Fatigue/Fracture, NDE, Materials and Manufacturing, Proc. Int. Conf. on Pressure Vessel Technology. New York (New York, USA): ASME 1996;1:125–46.

[4] Derenne M, Marchand L, Payne JR. Elevated temperature characterization of flexible graphite sheet materials for bolted flanged joints. Welding Research Council Bulletin 1997;419:1–86.

[5] Mueller RT. Recent buckling experiences with spiral wound flexible graphite filled gaskets. Computer Technology–1996: Applications and Methodology, American Society of Mechanical Engineers, Pressure Vessels and Piping Division. New York (New York, USA): ASME 1996;326:23–34.

[6] Crowley ED. Stemming leaks with spiral-wound gaskets. Chem Eng 1993;100(7):139–40.

[7] Crowley ED. Stemming leaks with spiral-wound gaskets. Chem Eng 1993;100(7):142.

[8] Jones WF, Seth BB. Replacing asbestos steam path gaskets. Power Eng 1992;96(3):43–5.

[9] Bazergui A, Winter JR. Room temperature and elevated temperature tests of a metal corrugated gasket with flexible graphite fill. American Society of Mechanical Engineers, Pressure Vessels & Piping Division. New York (New York, USA): ASME, 1989;158:33–40.

[10] Hirschvogel A. Sealed joints with regard to corrosive processes. Analysis of Bolted Joints, American Society of Mechanical Engineers, Pressure Vessels and Piping Division. Fairfield (New Jersey, USA): ASME, 1998;367:81–7.

[11] Chynoweth E. Seal of approval–graphite foil does the job safely. Process Engineering (London) 1987;68(7):63–4.

[12] Luo X, Chung DDL. Electromagnetic interference shielding reaching 130 dB using flexible graphite. Carbon 1996;34(10):1293–4.

[13] Tian J. Study on corrosion between flexible graphite and metal and its protection. Journal Wuhan University of Technology, Materials Science Edition 1995;10(1):53–60.

[14] Paul BO. Fire-safe stem packing meets emissions regulations. Chem Proc 1995;58(2):3.

[15] Hollerbach MA, Lee RL, Smith JP, Taylor PL. Upgrade of the DIII-D vacuum vessel protection system. Proc. Symp. Fusion Engineering, IEEE Service Center. Piscataway (New Jersey, USA) IEEE 1993;2:1185–8.

[16] Jones WF, Seth BB. Asbestos-free gasket materials for turbines. J Test Eval 1993;21(1):94–6.

[17] Corol W. Selecting asbestos-free gaskets. Eng Dig 1989;35(3):14.

[18] Corol W. Selecting asbestos-free gaskets. Eng Dig 1989;35(3):18–9.

[19] Childs P. Non-asbestos gaskets. Engineering 1988;228(11):3.

[20] Royse S. Assessing the limitations of non-asbestos gasket materials. Proc Eng 1988;69(9):73.

[21] Royse S. Assessing the limitations of non-asbestos gasket materials. Proc Eng 1988;69(9):75–6.

[22] Childs P. Non-metallic asbestos-free gaskets. Proc. Institution of Mechanical Engineers. Part A. Power & Process Engineering 1988;202(A1):63–8.

[23] Xu J. Flexible graphite and aluminium-impregnated graphite for liquid ammonia pumps sealing. Huagong Jixie/Chemical Engineering & Machinery 1987;14(1):14–8.

[24] Staaf E. Packing improves productivity in Swedish nuclear power stations. Nucl Plant J 1987;5(3):70.

[25] Staaf E. Packing improves productivity in Swedish nuclear power stations. Nucl Plant J 1987;5(3):72.

[26] Thomas S, McKillop GR. Substitute materials to replace asbestos in refinery-service gaskets and packings. Oil Gas J 1986;84(21):47–51.

[27] Petrunich PS. Gasket designs and applications using flexible graphite. SAE Technical Paper Series 830214. Warrendale (PA, USA):SAE, 12 p.